Journal of Sound and Vibration (2000) **236**(5), 881–894
doi:10.1006/jsvi.2000.3038, available online at http://www.idealibrary.com on IDEAL®

EFFECTS OF FILTERING THE ANGULAR MOTION OF THE CRANKSHAFT ON THE ESTIMATION OF THE INSTANTANEOUS ENGINE FRICTION TORQUE

H. K. Nehme, N. G. Chalhoub and N. A. Henein

Department of Mechanical Engineering, Wayne State University, Detroit, MI 48202, *U.S.A.*

(*Received* 11 *October* 1999, *and in final form* 22 *March* 2000)

The focus of this study is to investigate the effects of filtering the actual angular displacement, velocity and acceleration of the crankshaft on the computation of the instantaneous engine friction torque. These effects are isolated from those of measurement errors and/or noise by relying on a detailed model of the crank-slider mechanism to generate the rigid and flexible motions of the piston/connecting-rod/crankshaft mechanism along with the engine friction torque. The $(P-\omega)$ method is used herein to estimate the instantaneous engine friction torque based on the actual and the filtered angular displacement, velocity and acceleration of the crankshaft. The digital simulation results have demonstrated that the $(P-\omega)$ method cannot produce an acceptable estimation of the instantaneous engine friction torque in spite of filtering the actual angular motion of the crankshaft. It should be mentioned that the low-pass filter is commonly implemented to attenuate the measurement noise and the effects of structural deformations on the measured angular velocity of the crankshaft. However, the ineffectiveness of the low-pass filter stems from the non-linearities of the crank-slider mechanism that induced superharmonic and combination resonance frequencies in the angular displacement, velocity and acceleration of the crankshaft. The filter has severely attenuated some of the superharmonic resonance frequencies, which constitute an important part of the rigid-body behavior of the crankshaft that is needed by the $(P-\omega)$ method to accurately predict the engine friction torque. Moreover, the filtered signals would still be contaminated by the combination resonance frequencies that may appear in the low-frequency range commonly assumed to be dominated by the frequency components of the rigid-body motion of the crankshaft.

1. INTRODUCTION

Frictional losses of reciprocating and rotating engine components have a significant effect on the overall engine performance. Therefore, their effects should be adequately represented in the formulations of any engine model that is being developed for assessing the engine performance, particularly, under transient and high-speed modes of operation.

Common approaches for determining the average value of the overall frictional losses in internal combustion engines are the Willan line method, the Morse method and the indicated work method. Although these techniques consider engine firing conditions; however, they are limited in their scope of applications to steady state operating conditions [1].

Other methods such as the $(P-\omega)$ method [2] or the instantaneous mean effective pressure (IMEP) method [3] determine the overall instantaneous frictional losses of the engine and the instantaneous piston-assembly frictional losses respectively. Their

0022-460X/00/400881 + 14 $35.00/0

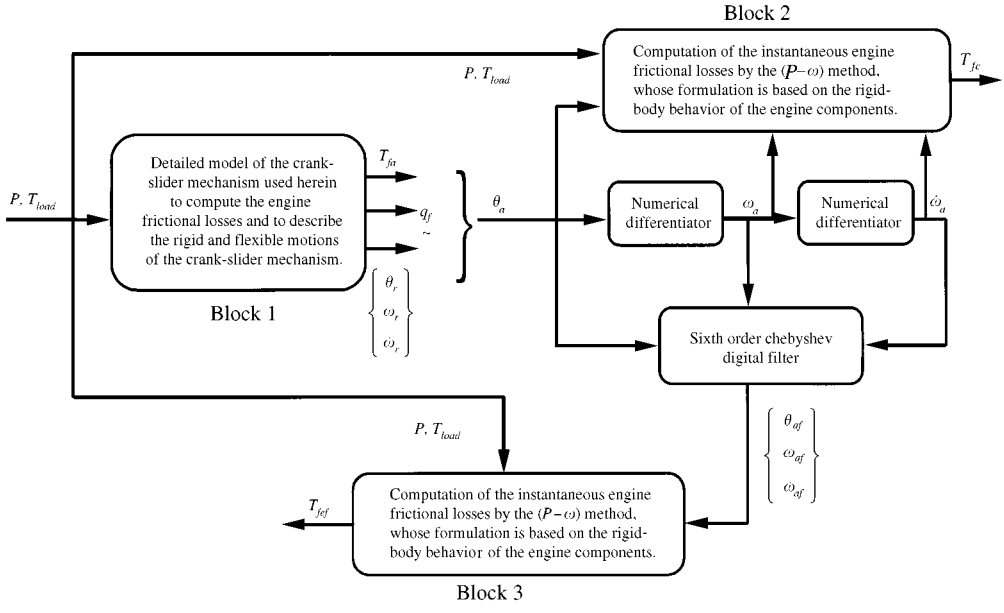

Figure 1. Strategy for assessing the effects of using filtered angular displacement, velocity and acceleration of the crankshaft in the computation of the instantaneous engine friction torque.

formulations account for the rigid-body behavior of the engine components and ignore the piston secondary motions along with the structural flexibility of the piston/connecting-rod/crankshaft mechanism. Conceptually, these two methods are applicable under transient and steady state modes of operation of the engine. Their implementation requires accurate measurements of the cylinder gas pressure, the connecting-rod forces and the crankshaft angular velocity. However, both the $(P - \omega)$ method and the IMEP method have yielded positive numerical values for the friction force/torque at specific periods during the engine cycle. The accuracy of these techniques depends heavily on the crank-slider model used in the computation of the frictional losses. The neglection of secondary motions of the piston and the structural deformations of the crank-slider mechanism from the formulations along with the improper interpretation of the measured connecting-rod forces and crankshaft angular velocity have rendered these techniques to be inaccurate, particularly at high engine speeds.

The focus of this work is to demonstrate the adverse effects induced by filtering the actual angular motion of the crankshaft on the computation of the instantaneous engine friction torque. To isolate these effects from those of measurement errors and/or noise, this work is conducted in the controlled environment depicted in Figure 1. A detailed model of the crank-slider mechanism is relied on to generate the rigid and flexible motions of the crankshaft/connecting-rod/piston mechanism and to determine the instantaneous engine friction torque. The $(P - \omega)$ method, used herein to estimate the friction torque, requires the rigid-body angular velocity of the crankshaft, ω_r, the cylinder gas pressure, P, and the engine load torque, T_{load}, as inputs. Barring any measurement errors, the difference between the actual crankshaft angular velocity, ω_a, and ω_r stems from the measurement noise and the contributions of the higher order dynamics of the system, namely, the structural deformations of the crank-slider mechanism. The common procedure for reducing the difference between ω_a and ω_r is to use a low-pass filter. Such a technique would be viable if

the frequency content of ω_r is clearly separated from those of the measurement noise and the higher order dynamics of the system. Unfortunately, the non-linear characteristic of the crank-slider mechanism causes ω_r to have super-harmonic resonant frequencies that are well within the frequency range of the elastic modes of the crankshaft. Thus, the use of a low-pass filter to attenuate the contributions of the higher order dynamics of the system from ω_a will ultimately result in a loss of significant frequency components from the rigid-body angular velocity of the crankshaft. Therefore, the objective of this work is to examine the effects of using filtered data in the $(P-\omega)$ method and to assess the impact of such a practice on the accuracy of the estimated engine friction torque, T_{fe}.

The detailed model of the crankshaft/connecting-rod/piston mechanism and the formulations for determining the frictional losses of the engine components are included in section 2. Subsequently, the digital low-pass filter and the differentiator are described. In section 4, the digital simulation results are presented. Finally, the work is summarized and the main conclusions are highlighted.

2. DYNAMIC MODEL OF THE CRANK-SLIDER MECHANISM

The distributed mass model, presented in this section, describes the combined rigid and flexible motions of the crankshaft/connecting-rod/piston mechanism for a single cylinder four-stroke internal combustion engine (see Figure 2). The derivation ignores the piston slap and the piston tilting. It treats the piston as a rigid body and computes the instantaneous friction torque, T_{fa}, based on the engine component friction formulations derived by Rezeka and Henein [4]. It should be emphasized that any other engine friction model could have equally served the purpose of this study.

The model takes into consideration the first three elastic modes for each of the torsional vibration, ϕ, and the out-of-plane transverse deformation, W_{CS}, of the crankshaft. Note that ϕ and W_{CS} are highly coupled. For any two adjacent beam elements of the crankshaft (see Figure 2), what may constitute the torsional vibration of one element becomes the slope of the transverse deformation of the other. The structural flexibility terms are discretized by using the assumed modes method [5]. The admissible functions in the ϕ and W_{CS} approximations are selected to be the eigenfunctions of the crankshaft, including the counterweights, the flywheel and the crank gear [6].

Since the connecting-rod is stiffer than the crankshaft then only the first elastic mode of its out-of-plane transverse deformation, W_{cr}, is included in the derivations. Similarly, the admissible function in the approximation of W_{cr} is considered to be the eigenfunction of a pinned-pinned beam, which is readily available in the literature.

The extended absolute position vectors of any point on the ith beam element of the crankshaft, the connecting rod as well as the mass center of the piston can be expressed as

$$\left\{\mathbf{r}_{CS}^{(i)\mathrm{T}} \,|\, 1\right\}^{\mathrm{T}} = \left[\prod_{j=1}^{i} T_{j-1}^{j}\right] T_{i}^{i'} \{x_{i'}\ y_{i'}\ 0 \,|\, 1\}^{\mathrm{T}}, \tag{1}$$

$$\left\{\mathbf{r}_{cr}^{\mathrm{T}} \,|\, 1\right\}^{\mathrm{T}} = T_{0}^{3}\, T_{\bar{3}}^{\bar{3}'}\, T_{\bar{3}'}^{6}\, T_{6}^{6'}\, \{0\ \ y_{6'}\ z_{6'} \,|\, 1\}^{\mathrm{T}}, \tag{2}$$

$$\left\{\mathbf{r}_{p}^{\mathrm{T}} \,|\, 1\right\}^{\mathrm{T}} = T_{0}^{3} T_{\bar{3}}^{\bar{3}'}\, T_{\bar{3}'}^{6}\, T_{6}^{6'_e}\, T_{6'_e}^{7}\, \{x_{7}^{*}\ y_{7}^{*}\ z_{7}^{*} \,|\, 1\}^{\mathrm{T}}. \tag{3}$$

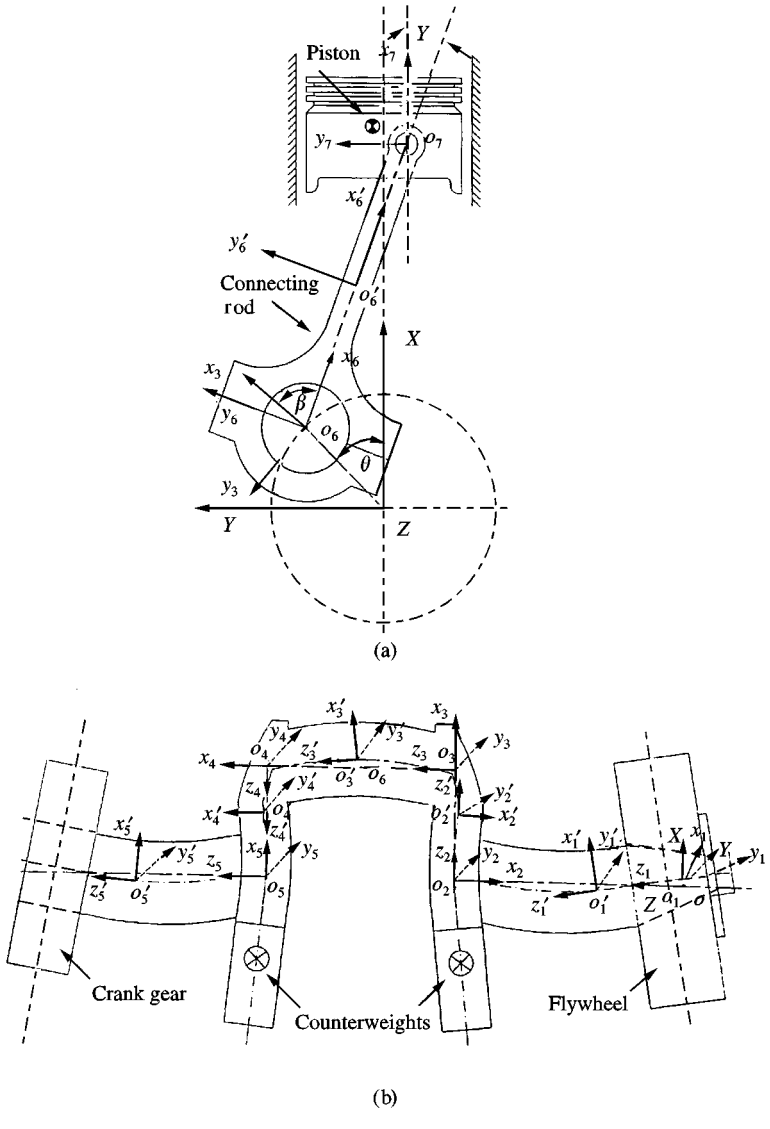

Figure 2. A schematic of the crank-slider mechanism: (a) connecting rod-piston, (b) crankshaft.

Next, the kinetic and potential energy expressions are determined from

$$KE = \frac{1}{2}\sum_{i=1}^{5}\int_{m_i}\dot{\mathbf{r}}_{CS}^{(i)}\cdot\dot{\mathbf{r}}_{CS}^{(i)}\,\mathrm{d}m_i + \frac{1}{2}\sum_{j}\left(m_j\dot{\mathbf{r}}_j\cdot\dot{\mathbf{r}}_j + \bar{\omega}_j^{\mathrm{T}}\,\bar{I}_j\bar{\boldsymbol{\omega}}_j\right) + \frac{1}{2}\int_{m_{cr}}\dot{\mathbf{r}}_{cr}\cdot\dot{\mathbf{r}}_{cr}\,\mathrm{d}m_{\mathrm{cr}}, \tag{4}$$

$$PE = \frac{1}{2}\sum_{i=1}^{5}\left[\int_0^{L_i} EI_i(W_{CS,z_iz_i})^2\,\mathrm{d}z_i + \int_0^{L_i} GJ_i(\phi_{,z_i})^2\,\mathrm{d}z_i\right] + \frac{1}{2}\int_0^{L_6} EI_6(W_{cr,\,x_6\,x_6})^2\,\mathrm{d}x_6$$
$$+ \sum_{i=1}^{5}\int_0^{L_i}\rho A_i g\,\mathbf{I}\cdot\mathbf{r}_{cs}^{(i)}\,\mathrm{d}z_i + \int_0^{L_6}\rho A_6 g\,\mathbf{I}\cdot\mathbf{r}_{cr}\,\mathrm{d}x_6 + \sum_j\left(m_j g\,\mathbf{I}\cdot\mathbf{r}_j\right),$$
$$j = fl,\ cw1,\ cw2,\ gr,\ p, \tag{5}$$

TABLE 1

Frictional losses of the engine components

Ring Boundary-mixed	$F_{rm} = 0{\cdot}252\,\pi D n_{crg} w_{crg}\,(P + P_{e,crg})(1 - \lvert\sin(\theta)\rvert)$ $270^\circ \leqslant \theta \leqslant 450^\circ$
Ring viscous lubrication	$F_{rv} = 23{\cdot}0\,[\mu \lvert V_p \rvert w_{crg}(P + P_{e,crg})]^{1/2}\,(1{\cdot}4\,n_{crg})D$
Skirt	$F_{sk} = \mu V_p D L_{skirt}/h$
Valve train	$F_{vt} = 0{\cdot}26\,n_{valve} SL/\sqrt{\dot{\theta}}$
Auxiliaries and unloaded bearings	$T_a = 9{\cdot}6\,\mu\dot{\theta}$
Loaded bearings	$T_{lb} = 0{\cdot}5(\pi/4)\,D^2\,P\,\lvert\cos(\theta)\rvert\,(d_1/2)/\sqrt{\dot{\theta}}$

where the datum line is considered to coincide with the inertial Z-axis (see Figure 2). The virtual work done by the nonconservative generalized force is

$$\delta W_{NC} = -PA_p\,\mathbf{I}\cdot\delta\mathbf{r}_p + \int_0^{L_2}\left\{\mathbf{F}_{ax}^{(2)}\cdot\left[-\frac{1}{2}\delta(W_{CS,z_2}^2)\,\mathbf{k}_2\right]\right\}\mathrm{d}z_2$$

$$+ \int_0^{L_4}\left\{\mathbf{F}_{ax}^{(4)}\cdot\left[-\frac{1}{2}\delta(W_{CS,z_4}^2)\,\mathbf{k}_4\right]\right\}\mathrm{d}z_4 + \int_0^{L_6}\left\{\mathbf{F}_{ax}^{(6)}\cdot\left[-\frac{1}{2}\delta(W_{cr,x_6}^2)\,\mathbf{i}_6\right]\right\}\mathrm{d}x_6$$

$$+ \delta W_f - T_{load}\,\mathbf{K}\cdot\left[-\delta W_{CS,z_5}\,\mathbf{i}_5 + W_{CS,z_5}\,\delta\theta\,\mathbf{j}_5 + (\delta\theta + \delta\phi)\mathbf{k}_5\right]_{z_5 = L_5}, \tag{6}$$

where the terms involving $\mathbf{F}_{ax}^{(i)}$ reflect the stiffening effect induced by the centripetal acceleration of the system. δW_f is the virtual work done by the friction forces and torques. It is defined as

$$\delta W_f = -(F_{rm} + F_{rv})\,\delta[T_0^7(x_{pr}^*\,y_{pr}^*\,z_{pr}^*\,|\,1)^{\mathrm{T}}] - F_{vt}\,\delta[T_0^7(x_7^*\,y_7^*\,z_7^*\,|\,1)^{\mathrm{T}}]$$

$$- F_{sk}\,\delta[T_0^7(x_{sk}^*\,y_{sk}^*\,z_{sk}^*\,|\,1)^{\mathrm{T}}] - (T_a + T_{lb})\left[\delta\theta + \frac{1}{2}\delta\phi\left(z_1 = \frac{L_1}{2}\right)\right.$$

$$\left. + \frac{1}{2}\delta\phi\left(z_5 = \frac{L_5}{2}\right)\right]. \tag{7}$$

The expressions for the friction forces and torques are adopted from the work done by Rezeka and Henein [4] (see Table 1).

Three co-ordinates θ, β and γ have been used herein to represent the rigid-body motion of the crank-slider mechanism. To deal with the superfluous coordinates, the following two constraint equations are imposed to prevent the piston from tilting or from moving away from the centerline of the cylinder in the **J** direction:

$$\bar{\boldsymbol{\omega}}_p\cdot\mathbf{k}_7 = 0 \quad \text{and} \quad \mathbf{r}_p^*(t)\cdot\mathbf{J} = \text{const.} \tag{8}$$

The equations of motion of the crank-slider mechanism are obtained by implementing the Lagrange principle. They can be written in the compact form

$$M(\mathbf{q})\,\ddot{\mathbf{q}} + \mathbf{F}(\mathbf{q}, \dot{\mathbf{q}}) = \mathbf{Q}^{NC} + s_1^{\mathrm{T}}(\mathbf{q})\,\boldsymbol{\lambda}, \tag{9}$$

where $\mathbf{q}$ is defined to be $(\theta, \beta, \gamma, q_1, q_2, q_3, q_4)^T$; s_1 is obtained by differentiating the constraint equations with respect to time and by writing the results as $s_1\ddot{\mathbf{q}} + \mathbf{s}_2 = \mathbf{0}$. The Lagrange multiplier vector, $\boldsymbol{\lambda}$, is determined by implementing the scheme in reference [7] and the equations of motion are integrated numerically by using the Gear's stiff integrator. The reader is referred to reference [6] for further details on the dynamic model of the crank-slider mechanism.

3. DIGITAL FILTER AND DIFFERENTIATOR

A low-pass filter is used in this study to significantly attenuate the high-frequency components in the crankshaft angular displacement, velocity and acceleration signals that are attributed to the structural flexibility of the crank-slider mechanism. Furthermore, the filter is designed such that signals with frequency contents well below the filter corner frequency would not undergo significant modifications in their magnitudes and phase shifts. After an elaborate search, a sixth order low-pass Chebyshev filter is found to yield the best compromise between an acceptable cut-off characteristic of the high frequency components and a reasonble phase shift [8]. The "cheby2" command line in MATLAB (general-purpose control software) is used in the design of the filter. The corner frequency was selected to be 520 rad/s while the sampling rate was 40 000 sample/s. The high sampling rate was chosen to enhance the resolution of the frequency spectrums for the filtered and unfiltered crankshaft angular velocity and acceleration. The z-domain transfer function of the digital filter can be expressed as

$$G_F(z) = \frac{(9{\cdot}78\, z^6 - 58{\cdot}38\, z^5 + 145{\cdot}5\, z^4 - 193{\cdot}8\, z^3 + 145{\cdot}5\, z^2 - 58{\cdot}38\, z + 9{\cdot}78) \times 10^{-5}}{z^6 - 5{\cdot}94\ z^5 + 14{\cdot}7\, z^4 - 19{\cdot}41\, z^{3+} + 14{\cdot}41\, z^2 - 5{\cdot}71\, z + 0{\cdot}94}. \tag{10}$$

Next, the MATLAB zero-phase forward and reverse digital filtering function "filtfilt" is used to eliminate phase distortions induced in the filtered signals by the filtering process.

A numerical differentiator based on the backward rule is implemented in this study to obtain the crankshaft angular velocity and acceleration. The z-domain transfer function of the differentiator can be expressed as

$$G_D(z) = \frac{1 - z^{-1}}{T_S}, \tag{11}$$

where T_S is the sampling period

4. DIGITAL SIMULATION RESULTS

The distributed mass model of the crank-slider mechanism, described in section 2, is included in block 1 of Figure 1. A cylinder gas pressure trace corresponding to engine firing conditions and a constant load torque are considered in this study. These signals are used in the detailed model to determine the overall friction torque of the engine, T_{fa}, and to predict the combined rigid and flexible motions of the crank-slider mechanism. The T_{fa} plot along with the rigid and flexible motions of the crank-slider mechanism are used herein as a base for comparison.

The $(P - \omega)$ formulation, which is based on the rigid body model of the crank-slider mechanism, is inserted in blocks 2 and 3 of Figure 1. In block 2, the $(P - \omega)$ method estimates the instantaneous engine friction torque based on the actual angular

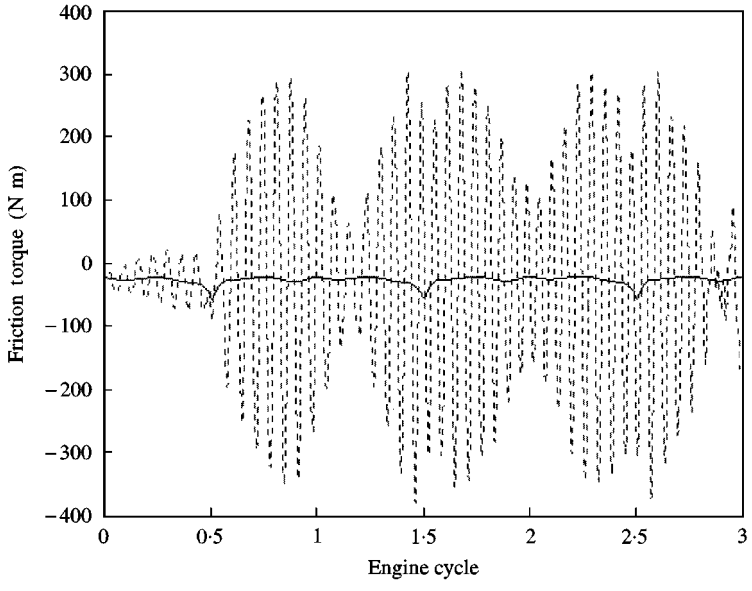

Figure 3. Instantaneous friction torque. ——, from a detailed model of the crank-slider mechanism, T_{fa}; - - -, from the $(P-\omega)$ method based on the actual angular displacement, velocity and acceleration of the crankshaft, T_{fe}.

displacement, velocity and acceleration of the crankshaft along with the cylinder gas pressure and the engine load torque (see Figure 1). The crankshaft angular displacement is usually measured by an optical encoder whose output signal θ_a represents both the torsional vibration and the rigid body angular displacement of the crankshaft, θ_r. ω_a and $\dot{\omega}_a$ are then obtained by differentiating the optical encoder signal with respect to time. In the noise-free environment depicted in Figure 1, the actual angular displacement of the crankshaft is simulated as

$$\theta_a = \theta_r + \sum_{i=1}^{3} \Phi_i(z_1 = 0)\, q_i(t). \tag{12}$$

By implementing the substitution method to eliminate the superfluous β and γ co-ordinates, the rigid-body model of the crank-slider mechanism can be reduced to the following differential equation in θ:

$$J(\theta)\,\ddot{\theta} + \bar{F}\,(\theta, \dot{\theta}) = G(P, T_{load}) + T_{fe}, \tag{13}$$

where all the frictional losses of the crank-slider mechanism have been lumped into a single term, T_{fe}. The measurements of θ, P and T_{load} along with the computation of the time derivatives of θ have rendered the terms in the above equation to become known quantities except for T_{fe}. Thus, the $(P-\omega)$ method treats equation (13) as an algebraic equation for estimating the instantaneous engine friction torque.

Figure 3 illustrates the plots for T_{fa} and the instantaneous engine friction torque, T_{fe}, which is estimated by the $(P-\omega)$ method based on the actual crankshaft angular displacement, velocity and acceleration as defined in equation (12). Given the noise-free environment of this study and the fact that the $(P-\omega)$ method does not account for the structural deformations of the crank-slider mechanism, then the large differences between T_{fa} and T_{fe} can only be attributed to the effect of the structural flexibility on θ_a, ω_a and $\dot{\omega}_a$. This argument has been carefully investigated in reference [9].

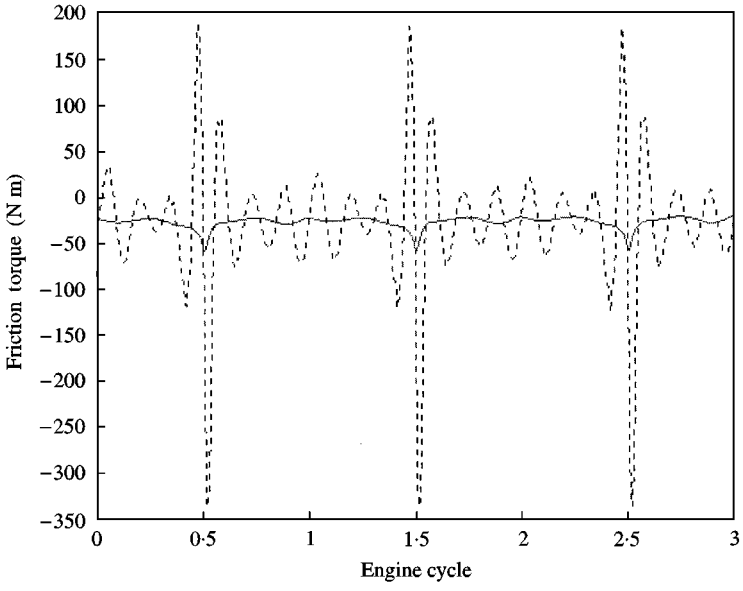

Figure 4. Instantaneous friction torque. ——, from a detailed model of the crank-slider mechanism, T_{fa}; - - -, from the $(P - \omega)$ method based on the filtered angular displacement, velocity and acceleration of the crankshaft, T_{fef}.

In block 3 of Figure 1, the $(P - \omega)$ method estimates the instantaneous engine friction torque based on the filtered angular displacement, velocity and acceleration of the crankshaft along with the cylinder gas pressure and the engine load torque. The rationale is to demonstrate the adverse effects of filtering θ_a, ω_a and $\dot{\omega}_a$ on the computation of the instantaneous engine friction torque.

Recall that the digital filter was carefully selected so that the low-frequency components of θ_a, ω_a and $\dot{\omega}_a$ are not attenuated. Furthermore, the MATLAB zero-phase forward and reverse digital filtering function "filtfilt" is used herein to eliminate any phase distortion of the signals due to the filtering process. Moreover, the cylinder gas pressure and the load torque used in calculating T_{fef} are exactly the same signals that were incorporated in the computation of T_{fa} and T_{fe}. The comparison of Figures 3 and 4 reveals that the process of filtering the crankshaft angular displacement velocity and acceleration has significantly improved the estimation of the instantaneous engine friction torque. This is because the filtered signals θ_{af}, ω_{af} and $\dot{\omega}_{af}$ represent more accurately the rigid-body angular displacement, velocity and acceleration of the crankshaft than θ_a, ω_a and $\dot{\omega}_a$ (see Figures 5 and 6). However, one should note that in spite of incorporating the filtering process, the $(P - \omega)$ method has still failed to yield an acceptable estimation of the friction torque because T_{fef} is shown in Figure 4 to take on large positive values in addition to being highly oscillatory.

The filtering process of the crankshaft angular displacement, velocity and acceleration signals is commonly relied on to attenuate the effects of noise and higher order dynamics of the system. The failure of this procedure in the current study is attributed to the non-linearities inherent in the crank-slider mechanism, which introduced superharmonic resonance frequencies $n\omega_0$, $n = 1, 2, \ldots,$ and combination resonance frequencies $\omega_{ni} \pm n\omega_0$ in θ_a, ω_a, $\dot{\omega}_a$. For instance, superharmonic resonance frequency components that are significantly contributing towards the rigid body behavior of the crankshaft may exist in the frequency range of the structural flexibility of the crank-slider mechanism (see Figure 7).

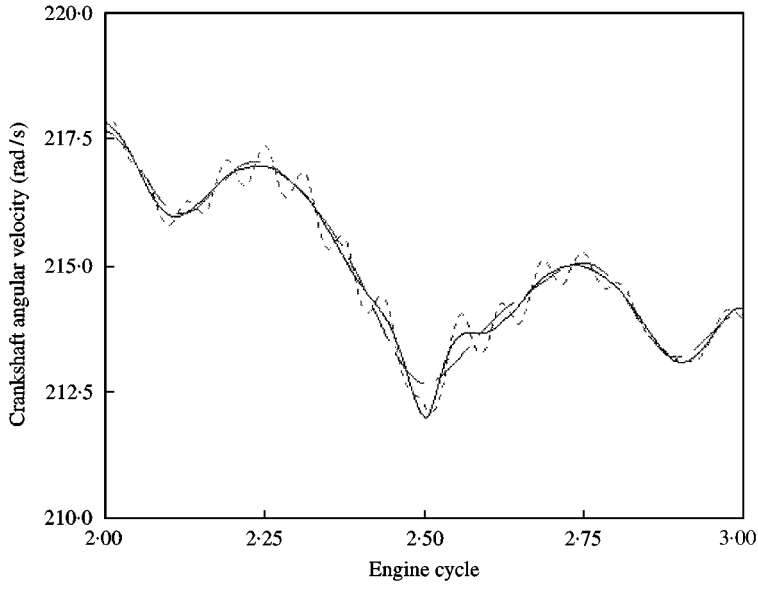

Figure 5. Angular velocity of the crankshaft. ——, rigid-body angular velocity, ω_r; – –, filtered angular velocity, ω_{af}; - - -, actual angular velocity, ω_a.

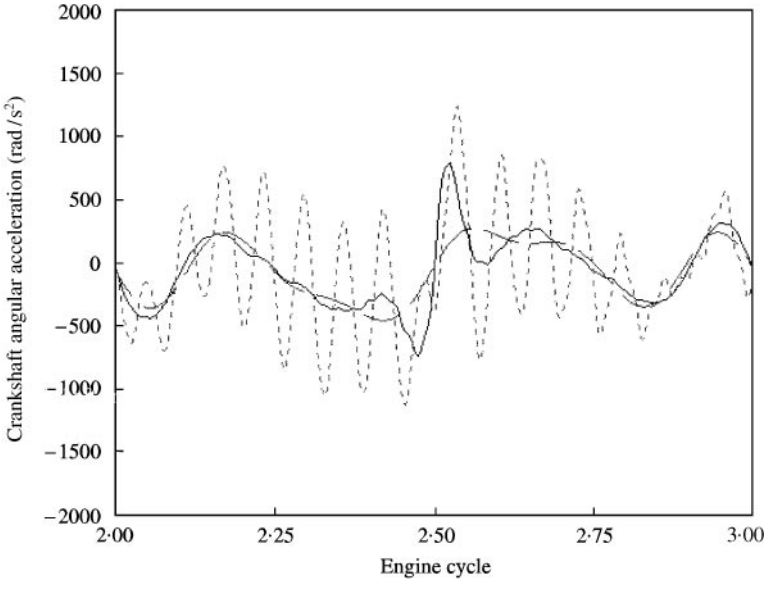

Figure 6. Angular acceleration of the crankshaft. ——, rigid-body angular acceleration, $\dot{\omega}_r$; – –, filtered angular acceleration, $\dot{\omega}_{af}$; - - -, actual angular acceleration, $\dot{\omega}_a$.

Similarly, combination resonance frequency components, $\omega_{ni} \pm n\omega_0$, may appear in the frequency range that is originally considered to be solely dominated by the frequency components of the rigid body motion of the crankshaft. This phenomenon prevents the filtered signals θ_{af}, ω_{af} and $\dot{\omega}_{af}$ from accurately representing θ_r, ω_r and $\dot{\omega}_r$ due to the severe attenuation of some of the superharmonic resonance frequencies, which constitute

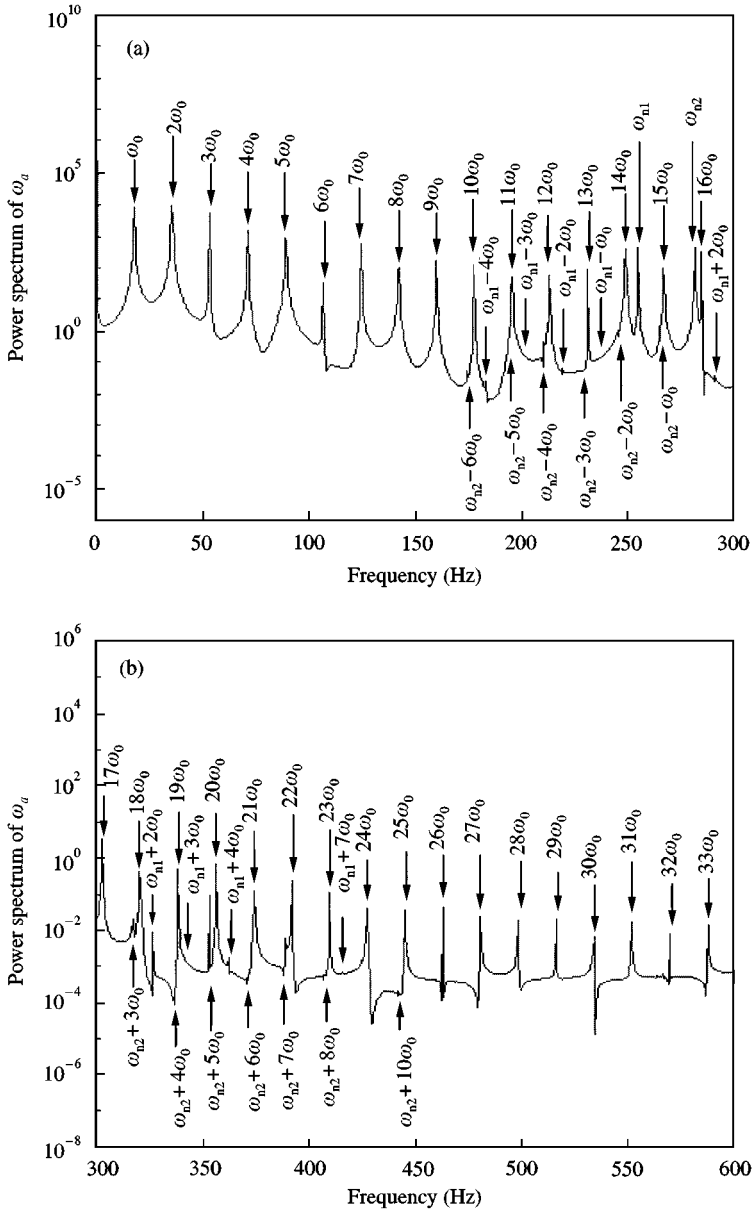

Figure 7. Frequency spectrum of the actual angular velocity of the crankshaft: (a) 0–300 Hz; (b) 300–600 Hz.

a significant component of the actual rigid body motion of the crankshaft. This is clearly manifested in Figures 5 and 6 by the large differences between ω_{af} and ω_r as well as between $\dot{\omega}_{af}$ and $\dot{\omega}_r$ in the vicinity of the top-dead-center position of the piston that occurs between the compression and the power strokes of the engine cycle. As a consequence, the largest error in the estimated friction torque, T_{fef}, has occurred during the same period in the engine cycle (see Figure 4). Furthermore, one should note that the filtered signals would still be contaminated by the combination resonance frequency components that may appear in the supposedly low frequency range of the rigid-body motion of the crankshaft. These

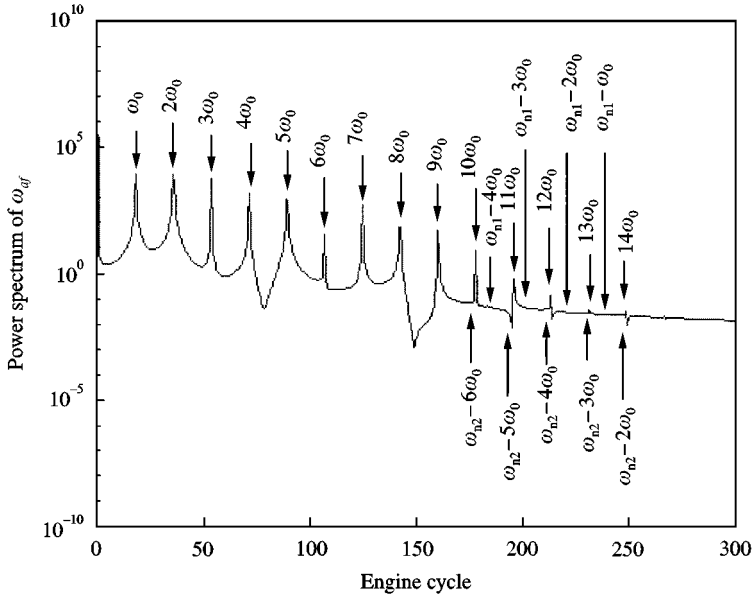

Figure 8. Frequency spectrum of the filtered angular velocity of the crankshaft.

effects are exhibited in the power spectrum of the filtered angular velocity of the crankshaft shown in Figure 8.

A comment is in order at this stage. At first glance, Figure 7 may give the wrong impression that only the superharmonic resonance frequency components are significant while the effects of the combination resonance frequencies can be ignored. It should be mentioned that Figure 7 represents the power spectrum of ω_a at steady state when the system is subjected to a cylinder gas pressure trace and a constant load torque. The cylinder gas pressure trace, used herein, is obtained experimentally for one engine cycle. The current work ignores cycle-to-cycle variations of P and applies the same pressure trace for all engine cycles that were considered in this study. To avoid the difficulties encountered by the stiff integrator in handling discontinuities that are inherent in the experimental data, the gas pressure trace was expressed in a Fourier series up to 48 terms. The discrete power spectrum of the cylinder gas pressure is expected to mostly excite the fundamental and the superharmonic resonance frequencies of ω_a. However, an actual pressure trace would have a continuous frequency spectrum that is capable of exciting the superharmonic and combination resonance frequencies of the system. Therefore, a better representation of P would be to treat it as a non-periodic signal; thus, taking into consideration cycle-to-cycle variations of the gas pressure and including several engine cycles in the computation of the Fourier transform of P.

It should be emphasized that the main conclusions of this work will not be affected whether only the superharmonic frequency components were excited or the superharmonic and combination resonance frequencies were excited simultaneously.

5. SUMMARY AND CONCLUSIONS

The present work investigates the effects of filtering the actual angular displacement, velocity and acceleration of the crankshaft on the computation of the instantaneous engine

friction torque. This study is performed in a fully controlled environment, depicted in Figure 1, that is free from any measurement errors or noise interference. A detailed model of the crank-slider mechanism for a single cylinder four-stroke engine is used as a test bed to generate the instantaneous engine friction torque and to determine the rigid and flexible motions of the crank-slider mechanism in response to the cylinder gas pressure and a constant load torque. The model takes into consideration the torsional vibration and the out-of-plane transverse deformation of the crankshaft along with the out-of-plane transverse deformation of the connection rod. In addition, the engine friction torque is determined based on the formulations provided by Rezeka and Henein [4] for the computation of the engine component frictional losses. It should be emphasized that any other engine friction model could have equally served the purpose of this study.

The $(P - \omega)$ method is used herein to estimate the instantaneous engine friction torque based on the actual θ_a, ω_a, $\dot{\omega}_a$ and the filtered θ_{af}, ω_{af}, $\dot{\omega}_{af}$ signals. The crankshaft angular displacement is commonly determined from an optical encoder signal, which reflects the contributions of the higher order dynamics of the system, the measurement noise and the rigid-body behavior of the crankshaft. A common procedure for attenuating the noise level and the unwanted contributions of the higher order dynamics is to use a low-pass filter. The current digital simulation results have demonstrated that the $(P - \omega)$ method can not produce an acceptable estimation of the instantaneous engine friction torque in spite of using the filtered signals θ_{af}, ω_{af} and $\dot{\omega}_{af}$. The reason is attributed to the non-linearities of the crankslider mechanism that have introduced superharmonic resonance frequencies $n\omega_0$, $n = 1, 2, \ldots$ and combination resonance frequencies $\omega_{ni} \pm n\omega_0$ in θ_a, ω_a and $\dot{\omega}_a$. The use of a low-pass filter causes severe attenuation in the superharmonic resonance frequencies, which constitute an important part of the rigid-body behaviour of the crankshaft that is needed by the $(P - \omega)$ method to accurately predict the engine friction torque. Moreover, the filtered signals would still be contaminated by the combination resonance frequency components that may appear in the low-frequency range commonly assumed to be dominated by the frequency components of the rigid-body motion of the crankshaft. Therefore, the non-linear characteristics of the crank-slider mechanism have rendered the low-pass filter to be ineffective in making θ_{af}, ω_{af} and $\dot{\omega}_{af}$ an accurate representation of the actual rigid-body behavior of the crankshaft.

Future work will now be focused on conducting experimental studies to validate the current theoretical results. Furthermore, a scheme for estimating the structural deformations of the crank-slider mechanism will be developed. The estimated flexible motion will then be used to extract the rigid-body motion for the actual angular displacement, velocity and acceleration of the crankshaft. The aim is to enhance the accuracy of the computed engine friction torque of the $(P - \omega)$ method through a better estimation of θ_r, ω_r and $\dot{\omega}_r$.

ACKNOWLEDGMENT

The authors would like to acknowledge the financial support of the Automotive Research Center (consortium of five universities directed by the University of Michigan) by the National Automative Center, located within the US Army Tank-Automotive Research, Development, and Engineering Center (TARDEC), Warren, Michigan.

REFERENCES

1. N. A. HENEIN 1992 *Technical Report*, *Mechanical Engineering Department*, *Wayne State University*. Instantaneous engine frictional torque, its components and piston assembly friction.

2. N. A. HENEIN, A. FRAGOULIS and A. NICHOLS 1988 *Journal of the Society of Tribologists and Lubrication engineers* **44**, 313–318. Time-dependent frictional torque in reciprocating internal combustion engines.
3. H. M. URAS and D. J. PATTERSON 1983 *SAE Paper* 830416. Measurement of piston and ring assembly friction instantaneous IMEP method.
4. S. F. REZEKA and N. A. HENEIN 1984 *SAE Paper* 840179. A new approach to evaluate instantaneous friction and its components in internal combustion engines.
5. L. MEIROVITCH 1986 *Elements of Vibration Analysis*. New York: McGraw-Hill.
6. H. NEHME, N. G. CHALHOUB and N. A. HENEIN 1998 *ASME Journal of Engineering for Gas Turbines and Power* **120-3**, 678–686. Development of a dynamic model for predicting the rigid and flexible motions of the crank slider mechanism.
7. C. GLOCKER and F. PFEIFFER 1992 *Nonlinear Dynamics* **3**, 245–259. Dynamical systems with unilateral contacts.
8. C. L. PHILLIPS and H. T. NAGLE 1990 *Digital Control System*: *Analysis and Design*. Englewood Cliffs, NJ: Prentice-Hall, second edition.
9. N. G. CHALHOUB, H. NEHME, N. A. HENEIN and W. BRYZIK 1999 *Journal of Sound and Vibration* **224-3**, 489–503. Effects of structural deformations of the crank-slider mechanism on the estimation of the instantaneous engine friction torque.

APPENDIX: NOMENCLATURE

A_i, m_i	cross-sectional area and mass of the ith beam element respectively
D, d_1	cylinder bore diameter and journal bearing diameter respectively
EI_i, GJ_i	flexural rigidity and torsional stiffness of the ith beam element respectively
F_{rm}, F_{rv}	represent the friction forces stemming from the boundary-mixed and the hydrodynamic lubrication regimes of the piston rings respectively
F_{sk}	friction force due to hydrodynamic lubrication regime of the piston skirt
F_{vt}	friction force of the valve train
$\mathbf{F}(\mathbf{q}, \dot{\mathbf{q}})$	vector containing inertial , stiffness and gravitational acceleration terms
$\bar{F}(\theta, \dot{\theta})$	represents inertial and gravitational acceleration terms in the rigid-body model of the crank-slider mechanism
$G(P, T_{load})$	non-conservative generalized forces due to the cylinder gas pressure and the load torque
g, ρ	gravitational acceleration and density respectively
h, $\bar{I}_j$	oil film thickness and inertia tensor of the jth rigid body respectively
$(\mathbf{I}, \mathbf{J}, \mathbf{K})$	unit vectors along the axes of the inertial co-ordinate system
$J(\theta)$	inertia term in the rigid-body model of the crank-slider mechanism
L_i, L_{skirt}	length of the ith beam element and the piston skirt respectively
$M(\mathbf{q})$	inertia tensor in the detailed model for the crank-slider mechanism
n_{crg}, n_{valve}	number of compression rings and valves respectively
P, $P_{e,\mathrm{crg}}$	cylinder gas pressure and elastic pressure of the compression ring respectively
$\mathbf{Q}^{NC}$	non-conservative generalized force vector
$\mathbf{q}_f$	vector containing the structural flexibility generalized co-ordinates $[q_1\ q_2\ q_3\ q_4]^{\mathrm{T}}$
SL, w_{crg}	valve spring load and average width of the compression ring respectively
T_a	friction torque of the auxiliaries and unloaded bearings
T_{fa}	engine friction torque generated by the detailed model of the crank-slider mechanism
T_{fe}, T_{fef}	engine friction torques generated by the $(P-\omega)$ method based on the actual θ_a, ω_a and $\dot{\omega}_a$ and the filtered θ_{af}, ω_{af} and $\dot{\omega}_{af}$ respectively
$T_i^{i'}$	represents the location of $O_{i'}$ and the orientation of $(x_{i'}, y_{i'}, z_{i'})$ with respect to (x_i, y_i, z_i)
T_{j-1}^{j}	4×4 matrix defining the origin and orientation of the jth co-ordinate system with respect to the $(j-1)$th frame in the nominal rigid-body configuration of the crankshaft
T_{lb}, T_{load}	friction torque of the loaded bearings and engine load torque respectively
V_p, μ	piston velocity and dynamic viscosity of the oil respectively
W_{cr}, W_{cs}	out-of-plane transverse deformations of the connecting-rod and the crankshaft respectively
$(x_{\bar{3}'}, y_{\bar{3}'}, z_{\bar{3}'})$	represents a floating co-ordinate system whose origin is fixed at $z_3 = L_3/2$
$(x_{6'_e}, y_{6'_e}, z_{6'_e})$	represents a floating co-ordinate system whose origin is fixed at $x_6 = L_6$

θ, β, γ,	angular displacements of the crankshaft, the connecting rod and the piston respectively
ϕ, Φ_i	torsional vibration and ith eigenfunction of the crankshaft
θ_a, ω_a, $\dot{\omega}_a$	actual angular displacement, velocity and acceleration of the crankshaft respectively
θ_{af}, ω_{af}, $\dot{\omega}_{af}$	filtered angular displacement, velocity and acceleration of the crankshaft respectively
θ_r, ω_r, $\dot{\omega}_r$	rigid-body angular displacement, velocity and acceleration of the crankshaft respectively
$\bar{\boldsymbol{\omega}}_j$	rotation vector of the jth rigid body
$()_{cr}$, $()_{cs}$	"*cr*" and "*cs*" subscripts refer to variables associated with the connecting-rod and the crankshaft respectively
$()_{cwi}$	a "*cwi*" subscript indicates a variable associated with the ith counterweight
$()_{fl}$, $()_{gr}$	"*fl*" and "*gr*" subscripts denote variables associated with the flywheel and the crank gear respectively
$()_p$, $()_{pr}$	"*p*" and "*pr*" subscripts refer to variables associated with the piston and the piston rings respectively
$()_{sk}$	a "*sk*" subscript refers to a variable associated with the piston skirt